Development of Positioning Technology Using LED

So-Hyeon Jo, Joo Woo, Sun Young Kim, *Member, IEEE*, and Jae-Hoon Jeong

***Abstract*—With the development of electric vehicles, indoor driving robots, wearable devices, etc., research on technology for recognizing one's current location continues to progress. Self-localization is an essential need for autonomous driving and mainly requires global positioning system (GPS), thereby using technologies such as LiDAR, Wi-Fi, and visible light communication (VLC). However, GPS is greatly affected by its surrounding environment, and it can make errors, especially in spaces where signals are blocked, such as tunnels and buildings. In this paper, we propose a system for estimating one's location using LED lights and frequency components with different color temperatures in an indoor space such as a tunnel. We installed three types of LED lights with different color temperatures in a tunnel-like experimental environment and collected data using RGB sensors. We also estimated the user's current location according to the color temperature and frequency component analysis from the data. In most cases, it was measured within a margin of error of 0–2 cm. It is expected that this will be used for generating data on the location of indoor service robots and autonomous vehicles in spaces where it is difficult to use GPS.**

***Index Terms*—Chromaticity, correlated color temperature (CCT), indoor positioning systems, LED.**

I. Introduction

With the development of satellite systems and the increased need for location information, the global navigation satellite system (GNSS) has become an essential technology. In the case of automobiles, global positioning system (GPS) has been used for a long time for navigation purposes. With the development of electric vehicles, the market size in various fields such as unmanned driving cars and indoor service robots, has increased. In the case of autonomous driving technology, it is one of the most important technologies to obtain information on the user's current location as the user does not interfere in the operation. Accordingly, various studies are actively researching methods to obtain location information [1].

Outdoors, users can easily obtain location information by receiving GPS signals through terminals such as smartphones, navigation devices, smartwatches, and tablets. In the case of indoor facilities or large cities with low signal strength, however, it is difficult to acquire location information, or it is obtained with errors because users can't efficiently receive signals. To improve the accuracy problem of GPS, many studies are currently trying to find various methods for indoor localization. With the increase in the use of smart devices and personal computers, various communication networks such as Bluetooth Low Energy(BLE) or Wi-Fi, 5G, and LTE have been built, and a method of estimating location through fingerprinting, and trilateration has been studied [2], [3], [4]. A map matching technology through the path passed by tracking back the track has also been studied [5]. Further efforts are currently developing technologies using cameras, radars, and LIDAR for location recognition through image processing. Also a technology recognizes location through reception sensitivity using sound and illumination [6], [7], [8], [9]. However, these methods are susceptible to interference from camera lenses and communication disturbances and require additional terminals.

Recently, many lights have been replaced with LEDs, which are highly efficient compared to conventional incandescent or fluorescent lamps, and their usage has increased rapidly [10]. Not only outdoor streetlights but also indoor lighting are being replaced by LEDs. Since the switching speed of LED is faster than the recognition speed of human beings, research is being conducted on a method for communication by loading data into light using this characteristic. Visible light communication (VLC) is becoming an alternative to the overload of the existing communication bandwidth, and it is relatively stable against electromagnetic interference. Accordingly, a location estimation technology based on light has been developed [11], [12], [13]. There are various measurement methods using VLC. Usually, each LED is assigned a unique ID. By giving various frequencies or pulse width modulations to the indoor ceiling led light, and using this as a marker, it showed sufficient accuracy at less than 50 cm [14], [15], [16], [17]. For situations where the dependence on LED lighting is not high, there is a method to design a DarkLight system to encode data into light pulses that are too short for humans to recognize [18], [19]. VLC system has high accuracy when using methods such as fingerprinting and signal strength, but the system configuration is a little complicated. For the proximity method, the system configuration is simple, but it is not rather accurate.

In this paper, we propose a technology for estimating position by analyzing the components of light measured according to location through LED lights with different color temperatures on a 2D plane. The gap between the LED chromaticity values used in the studies [20], [21], [22], [23], [24], [25] is reduced, and positioning is estimated through analysis using interpolation and FFT. Light changes color depending on its wavelength, and it can be obtained from the tristimulus values X, Y, and

Manuscript received 3 January 2023; revised 25 January 2023; accepted 26 January 2023. Date of publication 31 January 2023; date of current version 10 February 2023. This work was supported by the National Research Foundation of Korea (NRF) funded by the Korea Government (MSIT) under Grant NRF-2021R1F1A1052031. This work was also supported by the Research Funds of Kunsan National University. (*Corresponding authors: Joo Woo; Sun Young Kim; Jae-Hoon Jeong.*)

So-Hyeon Jo, Joo Woo, and Jae-Hoon Jeong are with the School of Software, Kunsan National University, Gunsan 54150, Republic of Korea (e-mail: shjo960@naver.com; whj9419@naver.com; jh7129@kunsan.ac.kr).

Sun Young Kim is with the School of Mechanical Engineering, Kunsan National University, Gunsan 54150, Republic of Korea (e-mail: sykim77@kunsan.ac.kr).

Digital Object Identifier 10.1109/JPHOT.2023.3240719

TABLE I
LIST OF ABBREVIATIONS

BLE	Bluetooth Low Energy
CCT	Correlated Color Temperature
CIE	Commission Internationale De l'Eclairage
FFT	Fast Fourier Transform
GNSS	Global Navigation Satellite System
GPS	Global Positioning System
LED	Light Emitting Diodes
VLC	Visible Light Communication

Z designated by the Commission Internationale de l´Eclairage (CIE) by measuring R, G, and B values. With these values, the chromaticity coordinates known as x and y on the chromaticity diagram can be calculated. The correlated color temperature (CCT) value can be obtained through x and y. As a result, information about the color temperature of the LED light can be obtained [20], [21], [22], [23], [24], [25]. The coordinates of the current location are estimated using the signals measured by the RGB sensor. Existing methods such as trilateration have complexity in infrastructure construction, such as having to assign individual ids to LEDs and considering the arrangement of LEDs. At least three id signals are required to estimate the position for a point. The method proposed in this paper only needs to consider the light of the LED itself input to the RGB sensor without such complexity. The main focus of this paper is as follows:

- Simplifies hardware and software configuration by enabling LED use without infrastructure configuration, such as imposing individual id for each LED
- Reduced sense of heterogeneity by narrowing the gap of the color temperature difference compared with previous studies
- Perform positioning by measuring with low point density over a wide range
- Positioning using CCT and FFT

The rest parts of the paper are organized as follows. In Section II, the color coordinates, black body, and correlated color temperature of light are described. The experimental environment configuration, system configuration, and experimental process are explained in Section III. The experiment and the result analysis according to the experiment are performed in Section IV. Section V presents a discussion and conclusion on the results of the system and experiment proposed in this paper. The list of abbreviations used in this paper is defined in Table I.

II. CHROMATICITY OF LIGHT

Light is located between the electromagnetic wave band of various wavelengths, and its color changes according to the ratio of the wavelengths. Among the wavelength bands of light, visible light has a range of about 380 to 750 nm. The closer the wavelength is to 380 nm (the short wavelength), the more purple it is. The closer the wavelength is to 750 nm (the long wavelength), the redder it is. The quantitative representation of color is called "color specification," and the light that causes the sensation of color in the eyes is the "color stimulus." In the case of the color stimulus, the colorimetric system expressed using the original stimuli R, G, and B is known as a "trichromatic system." A representative example of the trichromatic system is the CIE color model recommended by the International Commission on Illumination, which is defined as the RGB color system and the XYZ color system. In the case of XYZ, which is a tristimulus value, it can be obtained using RGB as follows [20], [22], [24], [26]:

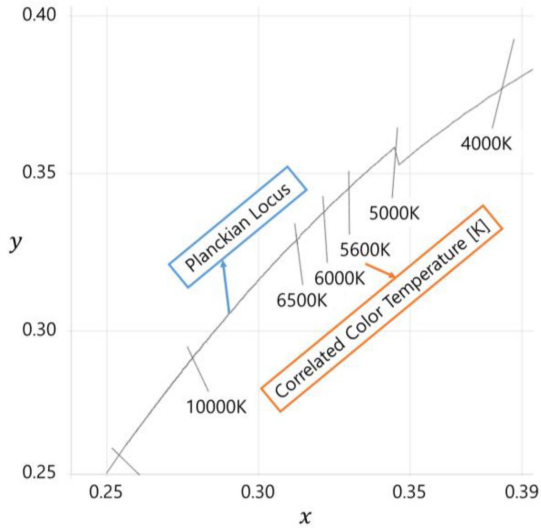

Fig. 1. Chromaticity coordinates with planckian locus and CCT.

$$\begin{bmatrix} \mathrm{X} \\ \mathrm{Y} \\ \mathrm{Z} \end{bmatrix} = \begin{bmatrix} 2.7689 & 1.7517 & 1.1302 \\ 1.0000 & 4.5907 & 0.0601 \\ 0.0000 & 0.0565 & 5.5943 \end{bmatrix} \begin{bmatrix} \mathrm{R} \\ \mathrm{G} \\ \mathrm{B} \end{bmatrix} \tag{1}$$

Blackbody radiation refers to the spectrum of light emitted by any heated object, and the absolute temperature of the blackbody corresponds to each color. This is defined as CCT. X, Y, and Z can be converted to the chromaticity coordinates (x, y) on a 2D plane as follows [27], [28]:

$$x = \frac{X}{X+Y+Z}, \; y = \frac{Y}{X+Y+Z} \tag{2}$$

The CCT value can be obtained through McCamy's formula and can be expressed as follows [29]:

$$\begin{aligned} &\mathrm{CCT} = 437\mathrm{n}^3 + 3601\mathrm{n}^2 + 6861\mathrm{n} + 5517 \\ &\text{where } \mathrm{n} = (\mathrm{x} - 0.3320) \,/\, (0.1858 - \mathrm{y}) \end{aligned} \tag{3}$$

Fig. 1 shows the relationship between the Planckian locus (Blackbody locus) and CCT on the chromaticity coordinates.

In this paper, we set up the experimental environment as shown in Fig. 2 and conducted localization experiments using LEDs with CCT characteristics in the white band [20], [21], [22], [23], [24], [25].

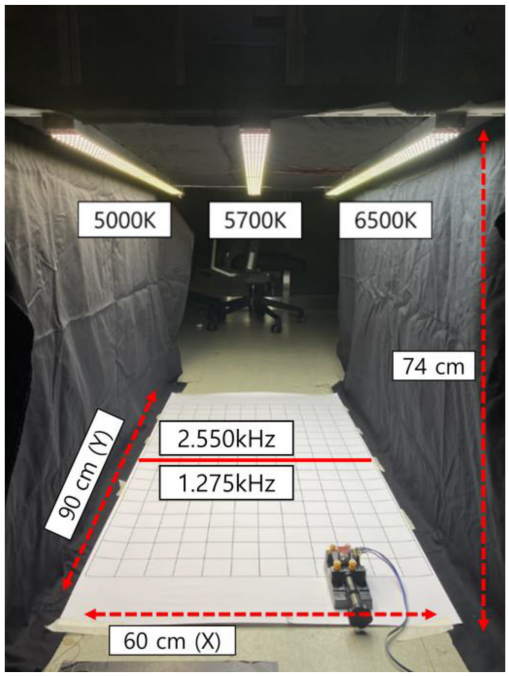

Fig. 2. Tunnel environment simulation for the experiment.

III. System Principle

A. Construction of Tunnel Simulator

In this study, long bar-type LED lights 5000 K, 5700 K, and 6500K were attached to be used as tunnel lighting. To reduce the visual heterogeneity of light, the LEDs belonging to the white band are arranged by reducing the color temperature gap. Each light is positioned at a height of about 74 cm from the floor to illuminate the measurement area, and the measurement area has a size of 60 cm × 90 cm in width and length. The RGB sensor for measuring the LED is fixed to the binder and moves the X-Position and Y-Position in the direction horizontal to the LED at about 5.7 cm from the floor. The coordinates of the X-Position (60 cm) were estimated by the change of color temperature using CCT values. Each LED bar is split in half (45 cm each) and driven at two frequencies. The coordinates of the Y-Position (90 cm) were estimated by the change in frequency sensitivity through FFT analysis.

As shown in Fig. 3, the LED signals are measured for R, G, and B values of each position using Arduino, RGB sensor, and MCP3204. Due to disturbance factors except for LED lights used for positioning, the signals measured by the RGB sensor may include distortion and bias of the waveform [20], [21], [22], [23], [24], [25]. As shown in Fig. 3, we designed a low-pass filter to remove the disturbance factors and transmit data.

To obtain CCT data, we measured seven sections at 10 cm intervals in the X-Position and four sections at 30 cm intervals in the Y-Position. R, G, and B values measured in each section were used to obtain X, Y, and Z values through (1), and X, Y, and Z values were used to obtain x and y values through (2). CCT and the element "n" required to obtain the CCT value, were obtained through x and y in (3).

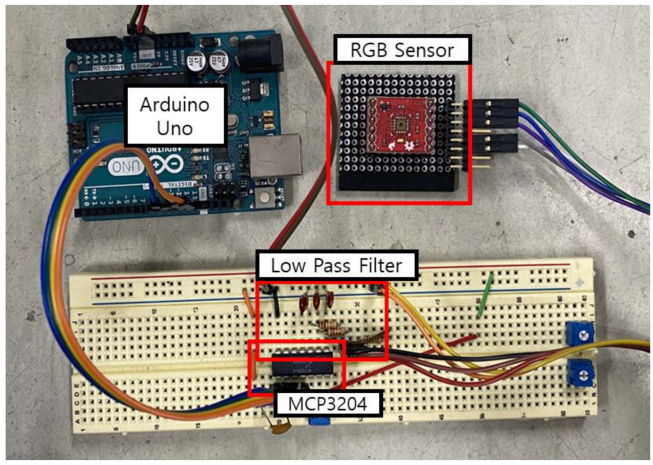

Fig. 3. Hardware configuration to obtain RGB data.

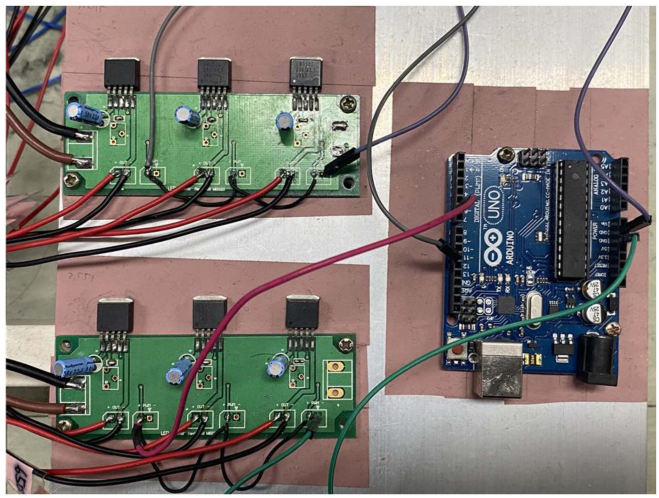

Fig. 4. LED driver to give the LED a frequency component.

To distinguish the position of the Y-Position, we divided LEDs into upper and lower parts and applied frequencies of 1.275 kHz and 2.550 kHz (each having a duty ratio of 50%). As shown in Fig. 4, we used an LED switching driver and an Arduino to separate and supply power. Additionally, we used an oscilloscope to check the frequency component as shown in Fig. 5 [20], [21], [22], [23], [24], [25].

The signal received through the RGB sensor was measured after being separated into an RGB signal for FFT_A and an RGB signal for FFT_B through FFT. FFT_A and FFT_B represent the FFT values for 1.275 kHz and 2.550 kHz. The sensitivity of the two signals is changed along the Y-Position. We obtained data on the Y-Position position by calculating the output according to the signals of FFT_A and FFT_B using (4) for the two signals. To obtain FFT data, we measured five sections at 15 cm intervals in the X-Position and seven sections at 15 cm in the Y-Position.

$$FFT_{AB} = \frac{FFT_A - FFT_B}{FFT_A + FFT_B} \tag{4}$$

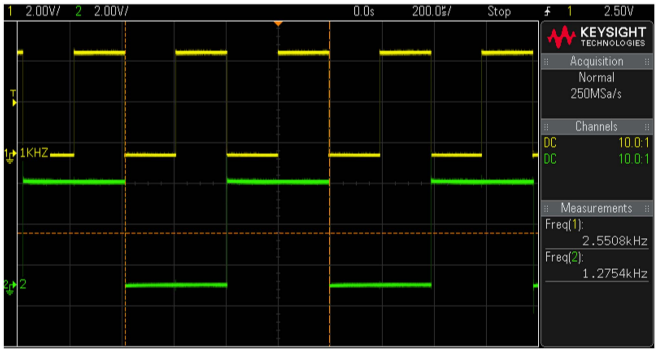

Fig. 5. Checking the frequency component applied to the LED using the oscilloscope.

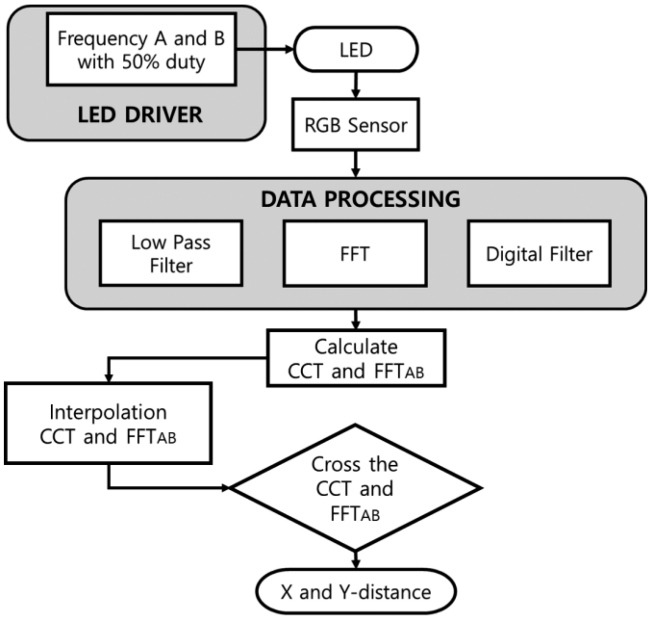

Fig. 6. System diagram for estimate X and Y-positions. B. Multipart Figures

The CCT and FFT values were compared according to location for coordinate estimation and the coordinates were estimated through the overlapping part of the two sections.

The overall flow of the system is shown in Fig. 6. The frequency component through LED driver is applied to the LED, and the RGB sensor measures the RGB value of the LED and proceeds with the data preprocessing process. The CCT and $\mathrm{FFT_{AB}}$ values obtained in this way specify the range according to the interpolated CCT and $\mathrm{FFT_{AB}}$, and the positions of X and Y-Position are estimated.

B. RGB Sensor Signal Processing Method

In Fig. 7(a) and (c), the coordinates of 4×7 CCT data and 7×5 $\mathrm{FFT_{AB}}$ data in 3D. The X-Position is the horizontal axis of 60 cm, and the Y-Position is the vertical axis of 90 cm. It can be seen that the CCT value increases as the X-Position approaches 60 cm, and the $\mathrm{FFT_{AB}}$ decreases as the Y-Position approaches 90 cm.

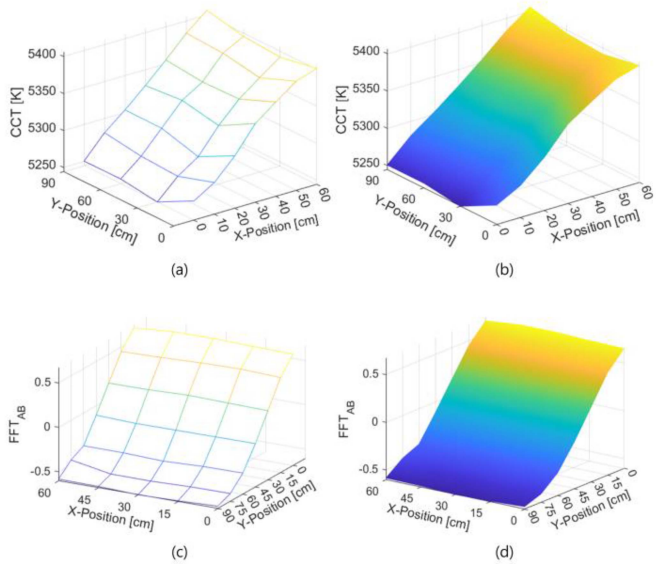

Fig. 7. Coordinates and interpolated coordinates for CCT raw and $\mathrm{FFT_{AB}}$. (a) 4×7 CCT raw data. (b) CCT interpolation data. (c) 7×5 $\mathrm{FFT_{AB}}$ raw data. (d) $\mathrm{FFT_{AB}}$ interpolation data.

TABLE II
PERCENTAGE OF THE GAP OF ERROR FOR ALL DATA

[cm]	0-1	1-2	2-3	3-4	4-5	over 5
X-Pos	44.13	15.79	13.36	8.10	5.67	12.96
Y-Pos	69.64	19.84	2.43	2.83	0.40	4.86

The data obtained through the experiment were interpolated using MATLAB to estimate the data for the section where there was no information about the location. Fig. 7(b) and (d) show the data with 2^8-1 interpolated points between sample values for (a) and (c).

If the CCT and $\mathrm{FFT_{AB}}$ distributed in a specific section are overlapped using interpolated data, the location information with the addresses of these two data can be extracted [29]. First, define the row and column sizes of the interpolated CCT and $\mathrm{FFT_{AB}}$ (sizeRows and sizeCols of (5), (6)), and store the interpolation interval information about how much space is interpolated at 60 cm and 90 cm (divRows and divCols of (5), (6)). After that, the difference between the maximum value and the minimum value within the interpolated data is calculated (7), and the interval to be extracted as much as the desired section is divided into this value (8). When information on input CCT and input $\mathrm{FFT_{AB}}$ are received through the RGB sensor using the above equations, a specific section is extracted from the CCT and $\mathrm{FFT_{AB}}$ information, and the information is stored (9).

$$\mathrm{divRows} = 90/\mathrm{sizeRows} \tag{5}$$

$$\mathrm{divCols} = 60/\mathrm{sizeCols} \tag{6}$$

$$\mathrm{Mag} = \mathrm{Max} - \mathrm{Min} \tag{7}$$

$$\mathrm{Div} = \mathrm{Mag}/\mathrm{div} \tag{8}$$

$$\mathrm{input} - \mathrm{Div} < \mathrm{output} < \mathrm{input} + \mathrm{Div} \tag{9}$$

TABLE III
THE AVERAGE FOR CCT AND FFT_{AB}, AND THE DEVIATION FOR EACH COORDINATE

x-axis	cm	0	5	10	15	20	25	30	35	40	45	50	55	60
y-axis	CCT_{avg}	5254	5265	5277	5291	5306	5318	5332	5348	5358	5370	5382	5391	5400
cm	FFT_{avg}	E	8.123	7.566	9.608	10.30	12.28	9.724	12.57	9.614	10.46	8.905	7.930	9.043	9.562
0	0.660	0.014	0.115	0.108	0.137	0.146	0.175	0.138	0.179	0.137	0.149	0.127	0.113	0.129	0.136
5	0.605	0.014	0.117	0.109	0.139	0.149	0.177	0.140	0.181	0.139	0.151	0.128	0.114	0.130	0.138
10	0.536	0.015	0.123	0.114	0.145	0.156	0.186	0.147	0.190	0.145	0.158	0.135	0.120	0.137	0.144
15	0.470	0.013	0.103	0.096	0.122	0.131	0.156	0.124	0.160	0.122	0.133	0.113	0.101	0.115	0.121
20	0.380	0.007	0.056	0.052	0.066	0.070	0.084	0.067	0.086	0.066	0.072	0.061	0.054	0.062	0.065
25	0.288	0.008	0.065	0.060	0.077	0.082	0.098	0.078	0.100	0.077	0.083	0.071	0.063	0.072	0.076
30	0.185	0.009	0.070	0.065	0.083	0.089	0.106	0.084	0.108	0.083	0.090	0.077	0.068	0.078	0.082
35	0.080	0.011	0.088	0.082	0.104	0.112	0.133	0.105	0.136	0.104	0.113	0.096	0.086	0.098	0.104
40	-0.024	0.014	0.114	0.106	0.135	0.144	0.172	0.136	0.176	0.135	0.146	0.125	0.111	0.127	0.134
45	-0.123	0.011	0.092	0.085	0.108	0.116	0.139	0.110	0.142	0.109	0.118	0.101	0.090	0.102	0.108
50	-0.215	0.014	0.116	0.108	0.137	0.147	0.176	0.139	0.180	0.138	0.150	0.127	0.113	0.129	0.137
55	-0.300	0.010	0.081	0.076	0.096	0.103	0.123	0.097	0.125	0.096	0.104	0.089	0.079	0.090	0.095
60	-0.375	0.007	0.057	0.053	0.067	0.072	0.086	0.068	0.088	0.067	0.073	0.062	0.055	0.063	0.067
65	-0.429	0.012	0.101	0.095	0.120	0.129	0.153	0.121	0.157	0.120	0.131	0.111	0.099	0.113	0.119
70	-0.479	0.010	0.082	0.076	0.096	0.103	0.123	0.098	0.126	0.097	0.105	0.089	0.080	0.091	0.096
75	-0.515	0.021	0.172	0.160	0.203	0.218	0.260	0.206	0.266	0.203	0.221	0.188	0.168	0.191	0.202
80	-0.542	0.026	0.214	0.199	0.253	0.271	0.323	0.256	0.331	0.253	0.275	0.235	0.209	0.238	0.252
85	-0.564	0.022	0.175	0.163	0.207	0.222	0.264	0.209	0.271	0.207	0.225	0.192	0.171	0.195	0.206
90	-0.582	0.033	0.272	0.253	0.322	0.345	0.411	0.326	0.421	0.322	0.350	0.298	0.266	0.303	0.320

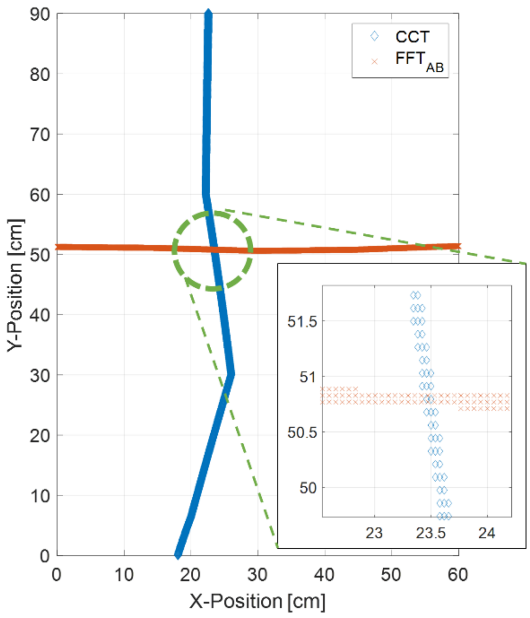

Fig. 8. Position estimation through the intersection of CCT and FFT_{AB}.

In Fig. 8, arbitrary CCT and FFT_{AB} values were input to show that the coordinates are estimated through (5)–(9). If CCT and FFT values are measured at a certain position, the blue diamond mark is the point marked for the interval where the measured CCT value exists. The red X mark is the point marked for the interval where the measured FFT_{AB} value exists. In other words, the range of the X-Position and Y-Position is founded on the input CCT value and the FFT_{AB} value. The coordinates of the current location are figured out through the data on the point where the two ranges overlap.

This was implemented using the look-up table and integrator in Simulink as shown in Fig. 9. The original data of CCT and FFT_{AB} is registered in the look-up table, respectively, and the coordinate position is figured out according to the input data using the integrator process. Using the look-up table saves runtime because there is no need to use equations. When the measured data is input to in_CCT and in_ FFT_{AB}, output values are displayed in the X-Position and the Y-Position. The input data were measured at intervals of 5 cm in width and length.

IV. EXPERIMENT AND ANALYSIS

To check the performance of the proposed position measurement system, a section of 60 cm × 90 cm was measured with an RGB sensor at 5 cm intervals, and CCT and FFT_{AB} values for a total of 247 coordinates were calculated. To visually check the coordinate estimation, specific coordinates are indicated on the graph as shown in Fig. 10.

Fig. 10 shows the output for the estimated position obtained through CCT and FFT_{AB} and the real position. The red circle represents the real coordinate, and the blue X represents the

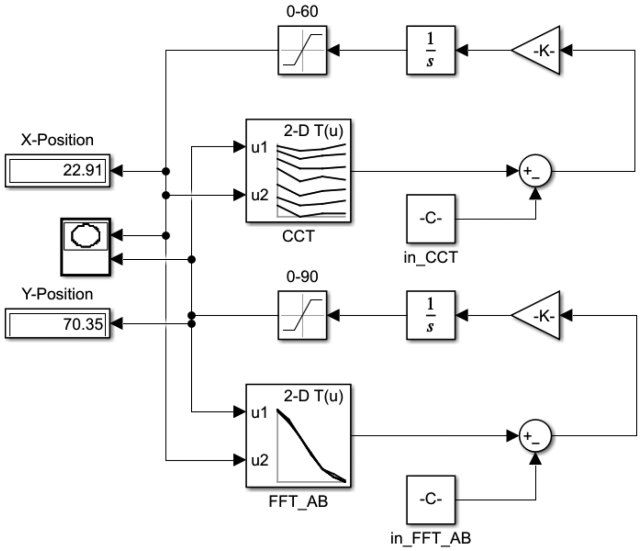

Fig. 9. Simulink design using the look-up table.

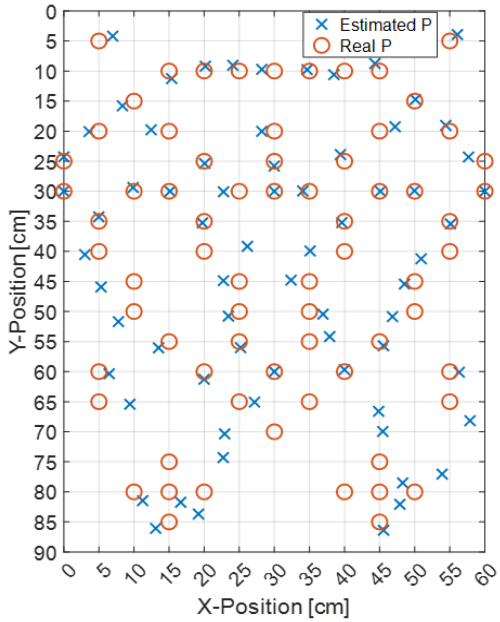

Fig. 10. Comparison of estimated position and real position.

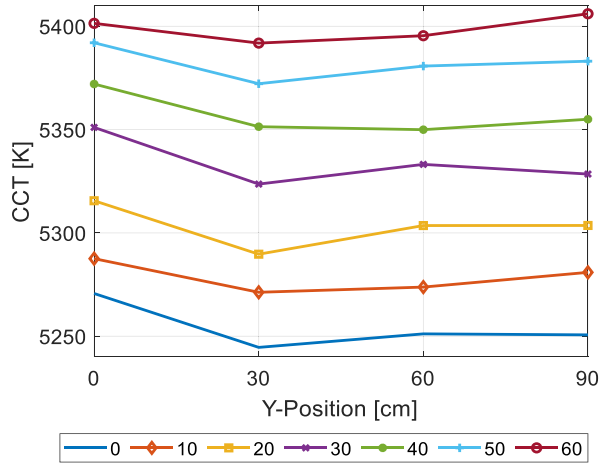

(a)

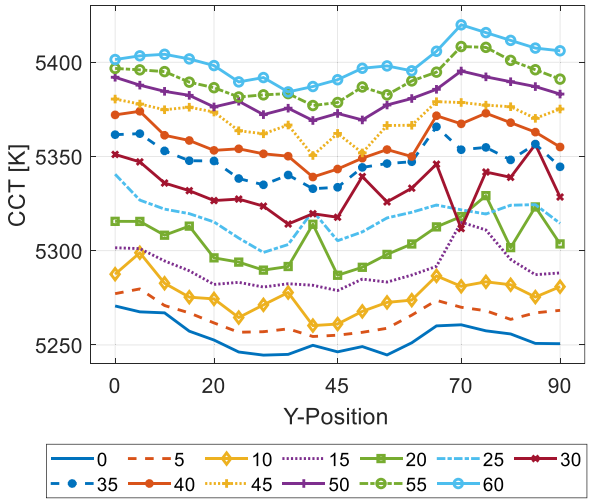

(b)

Fig. 11. CCT raw and CCT Full. (a) CCT raw values used for interpolation CCT_raw, (b) CCT values measured directly at 5 cm intervals used as in_CCT.

measured coordinate. Most of the outputs are within the 0–5 cm error range, and in particular, the error is insignificant for the Y-Position. Table II shows the percent error range for all data. Most of the data are distributed between 0 and 2 cm.

However, as the Y-Position approaches 90 cm, the X-Position margin of error increases. Table III shows the mean for CCT and $\mathrm{FFT_{AB}}$ obtained by measurement and the deviation for each coordinate.

Table III also shows that the deviation increases as the Y-Position approaches 90 cm. Comparing (a) and (b) in Fig. 11 can confirm the difference between the two graphs. Fig. 11(a) is the raw data of Figs. 7(a), and 11(b) is the CCT data measured per 5 cm. Unlike Fig. 11(a) showing a constant interval, Fig. 11(b) shows an unstable interval. This error value causes a large error in the coordinate estimation.

The reason for this error is that it is affected by the fluctuation of the LED itself as much as it depends on the LED light. During the experiment, the voltage and current of the power supply fluctuated somewhat, resulting in uneven LED output. In the case of the X-Position, since the RGB sensor uses the direct source output of the LED light, it is affected by the light condition. In the case of the Y-Position, the position is estimated by the relativity of the intensity of the frequency signal. For this reason, the effect of the light intensity is less, so the error seems to be relatively smaller than the X-Position.

When calculating the color temperature using the data obtained through the RGB sensor, we applied a digital filter to remove the DC component. However, due to the reflected LED light by the surrounding structures, the data is overlapped on the sensor and measured, so there is less accuracy in calculation. In addition, (1), used when converting RGB values into XYZ, is not a matrix tuned to the sensor and LED characteristics currently

used. The matrix required to convert RGB to XYZ requires reference white and chromaticity coordinate values of the RGB system. It is analyzed that the value came out inaccurate by using a matrix that did not go through a process to obtain this value. Therefore, follow-up research to reduce the effects of indirect is needed to conduct and reflected light and to set a matrix suitable for the system.

V. Conclusion

In this paper, we propose a method for estimating the current position through the color temperature and frequency ratio using LED with three color temperatures. The X-Position was estimated by analyzing the color temperature according to the X-Position through the LEDs with three color temperatures arranged along the Y-Position. The Y-Position was estimated by analyzing the sensitivity of two frequency components along the Y-Position. Position estimation was performed using data interpolation and Simulink using a look-up table, and the estimation results showed that the performance was close to the actual position. It reduced the sense of heterogeneity by narrowing the gap of the color temperature compared to previous studies and performed positioning by measuring with low point density over a wide range. It makes hardware and software configuration simplify. Currently, research on autonomous driving technology and indoor mobile devices is being actively conducted. In particular, if this technology is applied to a product to be operated indoors, it will be possible to estimate the location through a simple facility. This system can be deployed using the LED infrastructure that is basically installed in tunnels or indoor living facilities, and the need to maintain or repair each LED is reduced. In addition, it will be possible to further improve the system by reducing the disturbance caused by indirect and reflected light to minimize the position error and calculating the matrix adjusted for this system. After that, it is necessary to improve the performance by conducting additional experiments by reconfiguring the arrangement of LEDs and the experimental environment. Through this, it is expected that the location can be estimated through the positioning system using the LED platform in areas where GPS cannot reach and in places where communication interference is a concern.

References

[1] S.-U. Lee and S.-U. Kim, "Indoor positioning technology trends and prospects," *Inf. Commun. Mag.*, vol. 32, no. 2, pp. 81–88, 2015.

[2] I. Bisio et al., "A trainingless WiFi fingerprint positioning approach over mobile devices," *IEEE Antennas Wireless Propag. Lett.*, vol. 13, pp. 832–835, 2014, doi: 10.1109/LAWP.2014.2316973.

[3] B.-J. Shin, K.-W. Lee, S.-H. Choi, J.-Y. Kim, W.-J. Lee, and H.-S. Kim, "Indoor WiFi positioning system for android-based smartphone," in *Proc. IEEE Int. Conf. Inf. Commun. Technol. Convergence*, 2010, pp. 319–320.

[4] L. Bai, F. Ciravegna, R. Bond, and M. Mulvenna, "A low cost indoor positioning system using bluetooth low energy," *IEEE Access*, vol. 8, pp. 136858–136871, 2020.

[5] L. Zhihua and C. Wu, "A new approach to map-matching and parameter correcting for vehicle navigation system in the area of shadow of GPS signal," in *Proc. IEEE Intell. Transp. Syst.*, 2005, pp. 449–454.

[6] B. Lin, Z. Ghassemlooy, C. Lin, X. Tang, Y. Li, and S. Zhang, "An indoor visible light positioning system based on optical camera communications," *IEEE Photon. Technol. Lett.*, vol. 29, no. 7, pp. 579–582, Apr. 2017.

[7] M. Werner, M. Kessel, and C. Marouane, "Indoor positioning using smartphone camera," in *Proc. IEEE Int. Conf. Indoor Positioning Indoor Navigation*, 2011, pp. 1–6.

[8] J. Tiemann, F. Schweikowski, and C. Wietfeld, "Design of an UWB indoor-positioning system for UAV navigation in GNSS-denied environments," in *Proc. IEEE Int. Conf. Indoor Positioning Indoor Navigation*, 2015, pp. 1–7.

[9] S. Murata, C. Yara, K. Kaneta, S. Ioroi, and H. Tanaka, "Accurate indoor positioning system using near-ultrasonic sound from a smartphone," in *Proc. IEEE 8th Int. Conf. Next Gener. Mobile Apps Serv. Technol.*, 2014, pp. 13–18.

[10] C. Elliott, M. Yamada, J. Penning, S. Schober, and K. Lee, *Energy Savings Forecast of Solid-State Lighting in General Illumination Applications*. (No. DOE/EERE-2001), Washington, DC, USA: Navigant Consulting, Inc., 2019.

[11] M. S. Rahman, M. M. Haque, and K.-D. Kim, "Indoor positioning by LED visible light communication and image sensors," *Int. J. Elect. Comput. Eng.*, vol. 1, no. 2, pp. 161–170, 2011.

[12] P. H. Pathak, X. Feng, P. Hu, and P. Mohapatra, "Visible light communication networking and sensing: A survey potential and challenges," *IEEE Commun. Surveys Tuts.*, vol. 17, no. 4, pp. 2047–2077, Oct.–Dec. 2015.

[13] V. H. Al Khattat, S. B. Anas, and A. Saif, "An efficient 3D indoor positioning system based on visible light communication," in *Proc. 2nd Int. Conf. Emerg. Smart Technol. Appl.*, 2022, pp. 1–7.

[14] S. Yang, K. Kagemoto, and K. Onishi, "Coordinate detection for automatic guided vehicle using indoor ceiling LED lights," in *Proc. 5th IIAE Int. Conf. Ind. Appl. Eng.*, 2017, pp. 171–174.

[15] K. Kinoshitaa, S. Yanga, and S. Serikawaa, "Indoor location estimation using three photodiodes and ceiling LED lights," in *Proc. 7th IIAE Int. Conf. Intell. Syst. Image Process.*, 2019, pp. 173–177.

[16] G. Niu, J. Zhang, S. Guo, M. O. Pun, and C. S. Chen, "UAV-enabled 3D indoor positioning and navigation based on VLC," in *Proc. IEEE Int. Conf. Commun.*, 2021, pp. 1–6.

[17] C. W. Hsu et al., "Visible light positioning and lighting based on identity positioning and RF carrier allocation technique using a solar cell receiver," *IEEE Photon. J.*, vol. 8, no. 4, pp. 1–7, Aug. 2016, Art. no. 7905507, doi: 10.1109/JPHOT.2016.2590945.

[18] Z. Tian, K. Wright, and X. Zhou, "The darklight rises: Visible light communication in the dark," in *Proc. 22nd Annu. Int. Conf. Mobile Comput. Netw.*, 2016, pp. 2–15.

[19] C. Huang and X. Zhang, "Impact and feasibility of darklight LED on indoor visible light positioning system," in *Proc. IEEE 17th Int. Conf. Ubiquitous Wireless Broadband* , 2017, pp. 1–5, doi: 10.1109/ICUWB.2017.8250973.

[20] J.-H. Jeong, G. S. Byun, and K. Park, "Fuzzy logic vehicle positioning system based on chromaticity and frequency components of LED illumination," *IEEE Photon. J.*, vol. 11, no. 5, pp. 1–12, Oct. 2019, Art. no. 7906112.

[21] J.-H. Jeong and K. Park, "Numerical analysis of 2-D positioned, indoor, fuzzy-logic, autonomous navigation system based on chromaticity and frequency-component analysis of LED light," *Sensors*, vol. 21, no. 13, 2021, Art. no. 4345.

[22] J.-H. Jeong, D. H. Lee, G. S. Byun, H. R. Cho, and Y. H. Cho, "The tunnel lane positioning system of an autonomous vehicle in the LED lighting," *J. Korean Inst. Intell. Transp. Syst.*, vol. 16, pp. 186–195, 2017.

[23] J.-H. Jeong, M. Kim, and G. S. Byun, "Position recognition for an autonomous vehicle based on vehicle-to-led infrastructure," in *AETA 2016: Recent Advances in Electrical Engineering and Related Sciences; Lecture Notes in Electrical Engineering*, Berlin, Germany: Springer, 2017, pp. 913–921.

[24] J.-H. Jeong, G. S. Byun, and K. Park, "Tunnel lane-positioning system for autonomous driving cars using LED chromaticity and fuzzy logic system," *Electron. Telecommun. Res. Inst. J.*, vol. 41, pp. 506–514, 2019.

[25] J. Woo et al., "Determination of traffic lane in tunnel and positioning of autonomous vehicles using chromaticity of LED lights," *Sensors*, vol. 22, no. 8, 2022, Art. no. 2912.

[26] O. Noboru, *Introduction to Color Reproduction Technology*. Seoul, South Korea: JINSEM MEDIA, 2011.

[27] M. H. Brill, "Definition of chromaticity coordinates," *Color Res. Appl.*, vol. 39, no. 3, pp. 317–318, 2014.

[28] J.-S. B. Valencia, F.-E. L. Giraldo, and J.-F. V. Bonilla, "Calibration method for correlated color temperature (CCT) measurement using RGB color sensors," in *Proc. IEEE Symp. Signals Images Artif. Vis.*, 2013, pp. 1–6.

[29] C. S. McCamy, "Correlated color temperature as an explicit function of chromaticity coordinates," *Color Res. Appl.*, vol. 17, no. 2, pp. 142–144, 1992.

[30] S. H. Jo, J. Woo, G. S. Byun, and J. H. Jeong, "LED chromaticity-based indoor position recognition system for autonomous driving," in *Proc. Korean Inst. Inf. Commun. Sci. Conf.*, 2021, pp. 603–605.